HHS Public Access

Author manuscript

J Pathol. Author manuscript; available in PMC 2016 October 01.

Published in final edited form as:

J Pathol. 2015 October ; 237(2): 179–189. doi:10.1002/path.4573.

Genomic landscape of adenoid cystic carcinoma of the breast

Luciano G Martelotto[1], **Maria R De Filippo**[1], **Charlotte KY Ng**[1], **Rachael Natrajan**[2], **Laetitia Fuhrmann**[3], **Joanna Cyrta**[3], **Salvatore Piscuoglio**[1], **Huei-Chi Wen**[1], **Raymond S Lim**[1], **Ronglai Shen**[4], **Anne M Schultheis**[1], **Y Hannah Wen**[1], **Marcia Edelweiss**[1], **Odette Mariani**[3], **Göran Stenman**[5], **Timothy A Chan**[6], **Pierre-Emmanuel Colombo**[7], **Larry Norton**[8], **Anne Vincent-Salomon**[3,*], **Jorge S Reis-Filho**[1,*], and **Britta Weigelt**[1,*]

[1]Department of Pathology, Memorial Sloan Kettering Cancer Center, New York, NY, USA

[2]Breakthrough Breast Cancer Research Centre, The Institute of Cancer Research, London, UK

[3]Department of Tumor Biology, Institut Curie, Paris, France

[4]Department of Epidemiology and Biostatistics, Memorial Sloan Kettering Cancer Center, New York, NY, USA

[5]Sahlgrenska Cancer Center, Department of Pathology, University of Gothenburg, Gothenburg, Sweden

[6]Human Oncology and Pathogenesis Program, Memorial Sloan Kettering Cancer Center, New York, NY, USA

[7]Department of Surgical Oncology, Montpellier Cancer Institute (ICM), Montpellier, France

[8]Department of Medicine, Memorial Sloan Kettering Cancer Center, New York, NY, USA

Abstract

Adenoid cystic carcinoma (AdCC) is a rare type of triple-negative breast cancer (TNBC) characterized by the presence of the *MYB-NFIB* fusion gene. The molecular underpinning of breast AdCCs other than the *MYB-NFIB* fusion gene remains largely unexplored. Here we sought to define the repertoire of somatic genetic alterations of breast AdCCs. We performed whole exome sequencing, followed by orthogonal validation, of 12 breast AdCCs to determine the landscape of somatic mutations and gene copy number alterations. Fluorescence *in situ* hybridization and reverse transcription PCR were used to define the presence of *MYB* gene rearrangements and *MYB-NFIB* chimeric transcripts. Unlike common forms of TNBC, we found that AdCCs have a low mutation rate (0.27 non-silent mutations/Mb), lack mutations in *TP53* and

Correspondence to: Britta Weigelt, Department of Pathology, Memorial Sloan Kettering Cancer Center, 1275 York Avenue, New York, NY 10065, USA. Phone: +1 212-639-2332, Fax +1 212-639-2502, weigeltb@mskcc.org.

*These authors contributed equally for the supervision of the study.

AUTHORS' CONTRIBUTIONS

BW, AV-S and JSR-F conceived and supervised the study. LF, JC, OM, P-EC and AV-S provided and curated samples. AV-S and JSR-F performed the histopathologic review of cases. LGM, RN, LF, JC, JSR-F and AV-S carried out experiments and acquired data. LGM, MRDF, CKYN, RN, SP, H-CW, RSL, RS, AMS, YHW, ME, GS, TAC, LN, AV-S, JSR-F and BW analyzed and interpreted data. The first draft of the manuscript was written by LGM and BW, which was subsequently reviewed, edited and approved by all authors.

Conflict of interest: The authors have no conflicts of interest to declare.

PIK3CA, and display a heterogeneous constellation of known cancer genes affected by somatic mutations, including *MYB*, *BRAF*, *FBXW7*, *SMARCA5*, *SF3B1* and *FGFR2*. *MYB* and *TLN2* were affected by somatic mutations in two cases each. Akin to salivary gland AdCCs, breast AdCCs were found to harbor mutations targeting chromatin remodeling, cell adhesion, RNA biology, ubiquitination, and canonical signaling pathway genes. We observed that although breast AdCCs had rather simple genomes, they likely display intra-tumor genetic heterogeneity at diagnosis. Taken together, these findings demonstrate that the mutational burden and mutational repertoire of breast AdCCs are more similar to those of salivary gland AdCCs than to those of other types of TNBCs, emphasizing the importance of histologic subtyping of TNBCs. Furthermore, our data provide direct evidence that AdCCs harbor a distinctive mutational landscape and genomic structure, irrespective of disease site of origin.

Keywords

Adenoid cystic carcinoma; triple-negative breast cancer; genomics; *MYB-NFIB*; massively parallel sequencing

INTRODUCTION

Adenoid cystic carcinomas (AdCCs) are malignant tumors most commonly affecting the salivary glands, but can also be found in other anatomical sites including the breast, lungs and prostate[1]. AdCC of the breast is a rare (<1%) special histologic type of breast cancer that displays a triple-negative (i.e. estrogen receptor (ER)-negative, progesterone receptor (PR)-negative and HER2-negative) and basal-like phenotype[1-4]. Notably, breast AdCCs have an indolent clinical behavior, which is at variance with that of salivary gland AdCCs or common-type TNBCs (i.e. invasive ductal carcinomas of no special type, IDC-NSTs)[1,5]. Furthermore, while a subset of common-type TNBCs are sensitive to chemotherapy[5], it is thought that chemotherapy response rates in patients with breast AdCCs are low, akin to those observed in patients with salivary gland AdCCs[6,7].

AdCCs provide a clear example of genotypic-phenotypic correlation, as they display similar histologic characteristics irrespective of the site of origin and harbor the recurrent t(6;9)(q22-23;p23-24) translocation that results in the formation of the *MYB-NFIB* fusion gene[1,8]. The mechanistic basis for the oncogenic properties of this chimeric fusion gene, and in particular the role of the 3'-part of *NFIB*, has yet to be fully characterized. There is evidence, however, that this fusion gene results in activation and overexpression of MYB at mRNA and protein levels[1,8-10]. The prevalence of the *MYB-NFIB* fusion gene is reported to range from 28% to 100% in salivary gland AdCCs[8-13] and from 23% to 100% in breast AdCCs[8,9,14-16], however the clinical significance of this observation remains unclear. Although a substantial proportion of AdCCs lack the *MYB-NFIB* fusion gene, the majority of *MYB-NFIB* fusion gene-negative salivary gland AdCCs likely display activation of *MYB* due to mechanisms other than the t(6;9) chromosomal translocation[17].

Recent massively parallel sequencing studies have shown that common forms of triple-negative and basal-like breast cancers harbor recurrent *TP53* (50-80%) and *PIK3CA* (10%) mutations, and high levels of gene copy number alterations[18,19]. The molecular

underpinning of AdCCs of the breast other than the *MYB-NFIB* fusion gene remains largely unexplored, however. Our group has previously reported that a subset (12%) of breast AdCCs harbor mutations in *BRAF*[15], and that breast AdCCs display lower levels of genetic instability, as defined by gene copy number alterations, than basal-like IDC-NSTs[14,20]. The contribution of somatic mutations affecting other genes to the disease has yet to be determined.

The aims of our study were to define the landscape of somatic mutations and gene copy number alterations of breast AdCCs using whole exome sequencing, and to characterize the type and prevalence of *MYB* gene rearrangements and the respective *MYB-NFIB* chimeric transcript expression in these tumors.

MATERIALS AND METHODS

Case selection

Representative fresh/frozen and formalin-fixed paraffin-embedded (FFPE) tissues of 12 AdCCs of the breast were retrieved from the files of Institut Curie, Paris, France and Memorial Sloan Kettering Cancer Center (MSKCC), New York, USA. These cases had not been previously subjected to molecular analyses and have not been included in any previous study reported by our teams. All cases were centrally reviewed by two pathologists with an interest and expertise in breast pathology (AV-S and JSR-F). Tumors were classified according to the World Health Organization (WHO) criteria[3], and graded according to the Nottingham grading system[21]. This study was approved by the local ethics committees from the authors' institutions. Patient consents were obtained if required by the protocols approved.

Immunohistochemical analysis

Immunohistochemical analysis of the AdCCs was performed on representative 4 μm-thick FFPE sections, using antibodies against ER, PR and HER2 as previously described[22]. Positive and negative controls were included in each slide run[22]. Immunohistochemical results were evaluated by two pathologists (AV-S and JSR-F) according to the American Society of Clinical Oncology (ASCO)/College of American Pathologists (CAP) guidelines[23,24]. MYB protein expression was assessed by immunohistochemistry as previously described[25].

DNA and RNA extraction

The AdCCs included in this study contained >70% tumor cells after manual microdissection of the frozen specimen. Tumor sections were reviewed by pathologists under a stereomicroscope (Olympus SZ61) and surrounding healthy tissue was removed using a sterile needle. Genomic DNA was extracted from the tumor samples and matched normal tissue samples, confirmed by pathology review to be devoid of any neoplastic cells, using a standard phenol/chloroform-based protocol, and RNA was extracted from the tumor tissue using the RNeasy Mini Kit (Qiagen) according to the manufacturer's instructions. Nucleic acids were quantified using the Qubit Fluorometer assay (Life Technologies), and RNA integrity was defined using a Bioanalyzer (Agilent Technologies).

Fluorescence *in situ* hybridization (FISH)

The presence of the t(6;9)(q22-23;p23-24) translocation was investigated using the ZytoLight SPEC MYB Dual Color Break Apart Probe (Zytovision) following the manufacturer's instructions. Nuclei were counterstained using DAPI. Probes were visualized as red (Texas red) and green (FITC), and images were captured with a CDD camera, filtered and processed using a Leica Microsystems microscope. At least 50 interphase nuclei were analyzed per hybridization as previously described[14].

Reverse transcription (RT)-PCR and quantitative (q)RT-PCR

Standard end-point RT-PCR was performed in triplicate to detect the presence of the *MYB-NFIB* fusion transcripts, as previously described[8,9,16,22,26] (Supplementary Methods). qRT-PCR was performed to analyze the expression levels of 5' and 3' portions/exons of *MYB* using TaqMan Assay-on-Demand, as previously described[22] (Supplementary Methods).

Digital gene expression analysis

For qualitative analysis of the 5' to 3' expression ratio of *MYB* and *NFIB* mRNAs, 100ng of total RNA from each tumor sample was hybridized to a custom designed gene CodeSet (i.e. non-enzymatic RNA profiling using barcoded fluorescent probes; NanoString Technologies) using a validated protocol employed in the Integrated Genomics Operation (IGO) at MSKCC (Supplementary Methods, Supplementary Table S1).

Whole exome massively parallel sequencing

Matched tumor and normal DNA were subjected to whole exome capture (Agilent SureSelect Human All Exon v4) on an Illumina HiSeq 2000 using a validated protocol employed in the IGO at MSKCC, essentially as previously described[27]. For each sample, reads were aligned to the reference human genome GRCh37 using the Burrows-Wheeler Aligner (BWA, v0.6.2)[28]. Local realignment and quality score recalibration were performed using the Genome Analysis Toolkit (GATK, v3.1.1)[29]. De-duplication was performed using Picard (v1.92). Somatic single nucleotide variants (SNVs) were detected by MuTect (v1.1.4)[30], small somatic insertions and deletions (indels) by VarScan2 (v2.3.6)[31], Strelka[32] and Scalpel[33], and manually reviewed using the integrative genomic viewer (IGV)[34]. Variants found with >5% global minor allele frequency in dbSNP (Build 137) or that were supported by <5 reads were disregarded. SNVs for which the tumor variant allele fraction was <5 times than that of the normal variant allele fraction were disregarded as previously described[27]. Mutations were validated employing a targeted amplicon sequencing approach (Supplementary Methods). The potential functional effect of each SNV was assessed using previously described combination of mutation function predictors[35,36], as previously described[37] (Supplementary Methods). Validated mutations were functionally annotated into molecular pathways and networks, using the Ingenuity Pathway Analysis (IPA) software (http://www.ingenuity.com) and ConsensusPathDB-human[38] (Supplementary Methods).

To define the gene copy number alterations of breast AdCCs, whole exome sequencing data were analyzed using VarScan2[31] and GISTIC2.0[39]. In addition, ABSOLUTE was employed to infer tumor purity, tumor cell ploidy and clonal heterogeneity, as previously described[40].

Whole exome sequencing data have been deposited into the NCBI Sequence Read Archive, under accession code SRP053134.

Statistical analysis

Statistical comparisons between the mutation rates of *MYB-NFIB* fusion gene-positive and fusion gene-negative AdCCs, and between AdCCs and i) triple-negative and/or basal-like breast cancers and ii) salivary gland AdCCs were performed using the Mann-Whitney *U* test. Statistical analysis of qRT-PCR data was carried out using one-way ANOVA, Bonferroni's multiple comparison correction, alpha: 0.05. Two-tailed p-values were employed for all comparisons. Statistical analyses were performed using GraphPad Prism (v6.0f).

RESULTS

MYB-NFIB fusion gene prevalence and expression

All breast AdCCs included in this study were of triple-negative phenotype (i.e. lacked expression of ER, PR and HER2), of histologic grade 1 (58%) or grade 2 (42%), and composed of cribriform (17%), tubular-cribriform (67%), solid-cribriform (8%) or solid-trabecular (8%) growth patterns (Supplementary Figure S1; Supplementary Table S2). Consistent with previous reports[8,9,14-16], fluorescence *in situ* hybridization (FISH) and reverse transcription PCR (RT-PCR) analysis revealed that 10/12 breast AdCCs (83%) harbored the *MYB-NFIB* fusion gene (Table 1, Figure 1A, Supplementary Figure S2). Chimeric transcripts consisting of *MYB* exon 14 linked to *NFIB* exon 8c (n=6) or exon 9 (n=3) were most prevalent in the breast AdCCs analyzed, and in one case (AdCC2T) the fusion transcript consisted of *MYB* exon 9 linked to *NFIB* exon 8c (Table 1, Figure 1A, Supplementary Figures S2 and S3). Of note, due to alternative splicing and potentially variable breakpoints in *MYB* and *NFIB*, some breast AdCCs were found to express more than one *MYB-NFIB* transcript or splice variant (Figure 1A, Supplementary Figure S2), as previously described[8]. Using digital gene expression analysis (NanoString Technologies), we confirmed the elevated mRNA expression levels of the 5' portion of *MYB* and the 3' portion of *NFIB* in all ten *MYB-NFIB* fusion gene-positive breast AdCCs (Figure 1B). By contrast, the two *MYB-NFIB* fusion gene-negative breast AdCCs did not display elevated 5' *MYB* and 3' *NFIB* mRNA levels, but a pattern of expression similar to those of the *MYB-NFIB* fusion gene-negative ER-negative breast epithelial cell lines MCF10A and MCF12A and the ER-positive *MYB*-expressing breast cancer cell lines T47D and MCF7. Digital gene expression profiling and quantitative RT-PCR (qRT-PCR) further revealed that the overall *MYB* and 5' *MYB* mRNA expression levels in one of the fusion gene-negative tumors (i.e. AdCC12T) were significantly higher than in the remaining fusion gene-negative samples (i.e. case AdCC11T and breast cell lines) tested ($p<0.001$), but similar to those of *MYB* 5' exons of chimeric transcripts in *MYB-NFIB* fusion gene-positive breast AdCCs (Figure 1B

inset, 1C). These data suggest that *MYB* expression may be increased in AdCC12T due to a mechanism other than the *MYB-NFIB* rearrangement. Finally, the two breast AdCCs lacking the *MYB-NFIB* fusion gene did not show obvious histologic or clinico-pathologic differences as compared to the ten AdCCs harboring *MYB* rearrangements.

Spectrum of somatic mutations

We employed massively parallel sequencing to characterize the repertoire of somatic genetic alterations affecting the exomes of the 12 breast AdCCs included in this study. Tumor and matched normal DNA were subjected to whole exome sequencing, which resulted in a median sequencing depth of 78x (range 43-129x) and a mean of 88% of the target sequence covered to at least 10x depth (Supplementary Table S3). To ensure the accuracy of our massively parallel sequencing results, we performed an independent validation of the 181 candidate non-synonymous somatic mutations identified, including all single nucleotide variations (SNVs) and small insertions and deletions (indels), using targeted amplicon resequencing (see Methods; Supplementary Tables S4 and S5). As a result, we identified 167 non-synonymous somatic mutations affecting 160 genes in the 12 AdCCs of the breast analyzed here. The majority of validated somatic mutations identified in breast AdCCs were missense mutations (n=130), but nonsense mutations (n=18), essential splice site mutations (n=6), frameshift mutations (n=10), and in-frame indels (n=3) were also found as well as a total of 73 silent mutations (Supplementary Tables S4 and S5). A median of 12.5 mutations per tumor was found (range 6-23; Table 1, Supplementary Table S5), corresponding to an average of 0.27 non-silent mutations/Mb. Reanalysis of The Cancer Genome Atlas (TCGA) breast study[19] revealed that the exonic mutation rate of breast AdCCs was significantly lower than that of common forms of basal-like breast cancers (1.41 non-silent mutations/Mb; Mann-Whitney U-test, $p<0.001$) or TNBCs (1.38 non-silent mutations/Mb; Mann-Whitney U-test, $p<0.001$). In fact, the mutation rate found in breast AdCCs was more similar to that reported for pediatric malignancies[41] and salivary gland AdCCs (0.31 non-silent mutations/Mb; Mann-Whitney U-test, $p>0.1$)[12].

Mutational landscape of AdCCs of the breast

Common-type triple-negative and basal-like breast cancers are characterized by the presence of mutations targeting *TP53* and *PIK3CA* in 50%-80% and approximately 10% of tumors, respectively[18,19]. In addition, *ATM* mutations, *BRCA1* and *BRCA2* defects, and RB1 pathway deregulation have been described as being features characteristic of basal-like breast cancer[19]. In this study, we found a rather substantial heterogeneity in the landscape of somatic mutations in breast AdCCs. Importantly, unlike common-type triple-negative and basal-like breast cancers, no somatic mutations targeting *TP53*, *PIK3CA*, *RB1*, *BRCA1* or *BRCA2* were identified in breast AdCCs (Figure 2A; Supplementary Table S5).

We employed a combination of mutation effect prediction algorithms with a high negative predictive value[37], in combination with querying the presence of each mutated gene in the Cancer Gene Census[42], and/or in the list of cancer genes reported by Kandoth *et al*.[43] and Lawrence *et al*.[44] to discriminate passenger from potentially non-passenger mutations. This analysis resulted in the exclusion of 60 mutations, which were considered likely passengers, and in a list of 107 potentially non-passenger mutations, with at least one

potentially non-passenger somatic mutation per case (Supplementary Table S5). Several of these mutations affected known cancer-related genes including *BRAF*, *FBXW7*, *SF3B1*, *FGFR2*, *RASA1*, *PTPN11*, and *MTOR* (Figure 2A), suggesting that AdCC of the breast likely harbor potentially pathogenic mutations in addition to the *MYB-NFIB* fusion gene. Only two recurrent mutations were identified in the breast AdCCs studied here, two cases (AdCC2T and AdCC12T; 17%) harbored missense mutations affecting talin 2 (*TLN2*), a cytoskeletal protein that plays a role in actin filament assembly and cell migration, and two other cases (AdCC1T and AdCC32T; 17%) harbored missense mutations targeting *MYB* itself, where the mutation in case AdCC1T occurred in the exon 13 splice site of the *MYB* allele that is part of the actual *MYB-NFIB* fusion gene (Supplementary Figure S4). Whilst only one *BRAF* mutation was identified in the current series analyzed (8%), our group has previously reported the presence of *BRAF* mutations in 12% (3/25) of an independent cohort of breast AdCCs[15], providing evidence to suggest that *BRAF* may also be recurrently targeted by somatic mutations in these tumors.

Somatic mutations found in breast AdCCs affected genes either not mutated (e.g. *RASA1* or *PTPN11*) or mutated only in one of the basal-like breast cancers included in the TCGA dataset (e.g. *BRAF*, *FBXW7*, *SF3B1*, *FGFR2*, and *MTOR*, www.cBioPortal.org, accessed February 2015)[19,45]. On the other hand, 12 of the genes identified to harbor potentially non-passenger mutations in the breast AdCCs analyzed here were also found to be targeted by mutations in salivary gland AdCCs (12/107, 11.2% of genes affected by potentially non-passenger mutations; Figure 2A)[12,13]. The genes found to be commonly mutated between breast and salivary gland AdCCs comprised known cancer-related genes including *SF3B1*, *FBXW7*, *FGFR2*, *MYB* and *PRKD1* (Figure 2A, Supplementary Table S5)[12,13].

Despite the lack of recurrent mutations, annotation of the mutated genes identified in breast AdCCs revealed their convergence into several functional categories including chromatin remodeling and cell adhesion genes, akin to the genes mutated in salivary gland AdCCs[12,13], RNA biology, cell cycle/proliferation, ubiquitination/proteasome degradation, and neurogenesis/neuronal disorders (Figure 2A). Furthermore, pathway analysis of the genes affected by potentially non-passenger mutations in breast AdCCs using Ingenuity Pathway Analysis (IPA) and ConsensusPathDB revealed a significant enrichment for genes involved in the IGF1 and FGF signaling pathways (p-value<0.001), as reported for salivary gland AdCCs[12], and for genes related to the epithelial-mesenchymal transition (EMT) pathway (p-value<0.001) and Ephrin receptor signaling (p-value<0.001, Figure 2B). Taken together, our results suggest that the repertoire of somatic mutations of breast AdCCs is distinct from that of common forms of triple-negative and basal-like breast cancers but bears resemblance to that of salivary gland AdCCs.

Landscape of somatic gene copy number alterations

The exome sequencing data were also used to characterize the somatic gene copy number alterations of breast AdCCs. Consistent with previous observations by our group[14,20], breast AdCCs displayed low levels of genetic instability (Figure 3A), and no amplifications or homozygous deletions were identified. The most frequent copy number alterations were losses of 12q12-q14.1 in 5/12 cases (all *MYB-NFIB* fusion gene-positive) and gains of

17q21-q25.1 in 3/12 cases (two *MYB-NFIB* fusion gene-positive and one *MYB-NFIB* fusion gene-negative case, Figure 3A, Table 1, Supplementary Table S6). AdCCs of the breast were found to harbor a lower complexity in the pattern of gains and losses than that reported for common forms of triple-negative and basal-like breast cancers, and regions often altered in common-type TNBCs, such as 8q gain and 5q loss[19,46], were found not to be altered in breast AdCCs. In contrast, and consistent with the results of the mutational profiling, the landscape of gene copy number alterations found in breast AdCCs, including recurrent losses of 12q, was similar to that reported for salivary gland AdCCs[12,13,17,47].

Clonal heterogeneity

A subset of common forms of TNBC has been reported to display intra-tumor genetic heterogeneity at diagnosis[18]. Analysis of the clonal frequencies by integration of the gene copy number alterations and validated mutations identified in the breast AdCCs studied here using ABSOLUTE[40] revealed that the ploidy of all cases was ~2n (data not shown), and that many of the mutations identified were likely clonal with a cancer cell fraction >80% (Figure 3B). It should be noted, however, that a subset of mutations were likely subclonal with cancer cell fractions ranging from 9-79% (Figure 3B, Supplementary Table S5). These subclonal mutations also affected known cancer genes, such as *FBXW7, MTOR, MLL2 (KMT2D), ARAF* or *CDH1* (Figure 3C, Supplementary Table S5). These data provide evidence to suggest that although breast AdCCs have rather simple genomes, they may be composed of mosaics of cancer cells harboring subclonal mutations at diagnosis

DISCUSSION

Here we show that AdCCs of the breast, a rare type of TNBC, have a low exonic mutation rate, low levels of genetic instability, show a heterogeneous repertoire of somatic genetic alterations, and, in addition to the *MYB-NFIB* fusion gene, harbor mutations targeting chromatin remodeling, cell adhesion, and canonical signaling pathway genes including known cancer genes such as *BRAF, FBXW7, FGFR2* and *MTOR*. Furthermore, we observed that mutations and copy number alterations characteristic of common-type basal-like and TNBCs, such as mutations affecting *TP53* and *PIK3CA*, and 5q losses and 8q gains[18,19,46], are not found in breast AdCCs. On the other hand, AdCCs of the breast were found to harbor mutations in genes rarely mutated in basal-like breast cancers, including *RASA1, PTPN11* or *BRAF*, and recurrent 12q losses. Importantly, recurrent losses of 12q and somatic mutations affecting *SF3B1, MYB, PRKD1* and *FGFR2* have been documented in salivary gland AdCCs[12,13,17,47]. These results provide evidence to support the contention that breast AdCCs are more similar to salivary gland AdCCs than to common forms of triple-negative and basal-like breast cancers, and that TNBC is a mere operational term, encompassing a spectrum of lesions with distinct histologic features, clinical behaviors, and genomic landscapes[4,48]. In fact, contrary to common forms of TNBCs, patients with breast AdCCs have a favorable outcome[1,3,4,47].

Our genomic analysis of breast AdCCs has uncovered multiple alterations affecting known cancer genes and the involvement of several canonical signaling pathways that may play a role in their development. In addition to MYB overexpression, not driven exclusively by the

MYB-NFIB fusion gene, we observed that chromatin remodeling, cell adhesion/migration, RNA biology and neurogenesis-related genes were targeted by potentially pathogenic somatic mutations in breast AdCCs. Although only two genes (i.e. *MYB* and *TLN2*) were recurrently mutated in the 12 breast AdCCs studied here, annotation of the mutated genes in functional pathways and networks provided evidence to suggest that the mutations in AdCCs converged and preferentially affected genes involved in EMT, Ephrin receptor signaling, and IGF1 and FGF signaling pathways.

Given that AdCCs irrespective of the anatomical site are characterized by similar histologic features and the presence of the *MYB-NFIB* fusion gene[1,8], which was present in 83% of cases studied here, it is not entirely unexpected that some of the genes and signaling pathways reported to be targeted by mutations in salivary AdCCs are also affected in breast AdCCs. Breast and salivary gland AdCCs displayed many similarities in regards to their constellation of somatic genetic alterations, including similar mutation rates (0.27 non-silent mutations/Mb in breast vs. 0.31 non-silent mutations/Mb in salivary gland AdCCs[12]), recurrent losses of 12q, mutations affecting *SF3B1*, *FBXW7*, *FGFR2*, *MYB* and *PRKD1*, and enrichment for mutations affecting genes playing a role in chromatin remodeling, cell adhesion, and the FGF signaling pathway[12,13]. It should be noted, however, that at the genomic level, differences between the AdCCs of the breast and the salivary gland were also observed; whilst salivary gland AdCCs were reported to harbor mutations in *NOTCH1* and/or *NOTCH2*, and in *SPEN*[12,13], a downstream effector of NOTCH signaling, these genes were not found to be altered in breast AdCCs. Another important distinction between breast and salivary AdCCs relates to the enrichment for mutations affecting DNA damage response signaling genes in the latter but not in the former[12]. Using a binomial distribution, based on a reported 30% mutation rate in DNA damage response and NOTCH signaling pathway related genes in salivary gland AdCCs[12,13], the probability of observing at least one mutation in these genes in the 12 breast AdCCs analyzed here was 98.6% (Supplementary Methods), rendering a type II or β error unlikely. Taken together, although breast AdCCs appear to be more similar to AdCCs of the salivary glands than to triple-negative and basal-like breast cancers, important differences are also observed between breast and salivary gland AdCCs. Further studies are warranted to confirm these findings in larger series and to define whether these genetic differences may account for the reported distinct behaviors of AdCCs of the breast and salivary glands[1].

Despite the low level of genetic instability observed in breast AdCCs, our results provide evidence to suggest that in a way akin to other forms of cancer[18,49,50], at diagnosis, AdCCs may be constituted by a mosaic of cancer cell clones, with some potentially non-passenger mutations affecting known cancer genes being restricted to minor subclones within the tumor bulk. Although the biological and clinical significance of this observation remains to be fully elucidated, our findings demonstrate that even tumors with low levels of genetic instability may display intra-tumor genetic heterogeneity.

This study has several limitations. First, given the rarity of breast AdCCs (approximately 0.1% of all invasive breast cancers)[3,4], the number of cases analyzed here is relatively small. It is noteworthy, however, that the current study represents the largest cohort of breast AdCCs subjected to massively parallel sequencing to date. Second, the use of normal breast

tissue as the source of germline DNA for massively parallel sequencing analyses may lead to false-negative results. To ensure the absence of contaminating tumor cells in normal breast tissue, however, only normal tissue distant from the lesion was used, and the normal breast tissue was reviewed by pathologists and microdissected if required to be entirely devoid of any neoplastic cells. Third, the mutational signatures[51] in the *MYB-NFIB* fusion gene-driven cancers could not be studied given the limited number of somatic mutations present in a given breast AdCC. The development of breast AdCC cell lines or ER-negative non-malignant breast epithelial cell lines harboring the *MYB-NFIB* fusion gene may be required to elucidate the mechanistic basis of the oncogenic properties of the *MYB-NFIB* fusion gene, and the contribution of somatic genetic alterations other than the *MYB-NFIB* fusion gene for the tumorigenesis of these rare forms of TNBC. Furthermore, whole genome sequencing analysis of *MYB-NFIB* fusion gene-negative AdCCs is warranted to define alternative genetic mechanisms resulting in MYB overexpression and activation.

In conclusion, our findings demonstrate that at the genomic level, breast AdCCs are similar to salivary gland AdCCs and are likely distinct from common types of triple-negative or basal-like breast cancers. Our results provide further evidence of the heterogeneity of triple-negative and basal-like breast cancers at the molecular level, and that histologic subtyping of triple-negative/basal-like breast cancers provides useful information. In fact, our findings emphasize the importance of histologic subtyping in the context of triple-negative disease, given that breast AdCCs have outcomes and response to chemotherapy distinct from those of common forms of TNBC, and that agents targeting the driver genes most frequently mutated in common forms of TNBC may be of limited value for patients with breast AdCCs, given their distinctive repertoire of somatic mutations and gene copy number alterations. Finally, owing to the heterogeneity of TNBCs, their sub-stratification according to histologic and molecular subtypes may be required for the identification of disease drivers and therapeutic targets[48].

Supplementary Material

Refer to Web version on PubMed Central for supplementary material.

Acknowledgments

FINANCIAL SUPPORT

RN is funded by a Breast Cancer Campaign Career Development Fellowship (2011MaySF01), SP by a Susan G Komen Postdoctoral Fellowship Grant (PDF14298348), and AMS by a stipend from the German Cancer Aid (Dr. Mildred Scheel Stiftung). AV-S is supported by an Interface INSERM grant, and GS by the Swedish Cancer Society and BioCARE (University of Gothenburg). This study was funded in part by the Adenoid Cystic Carcinoma Research Foundation. Research reported in this publication was supported in part by the Cancer Center Support Grant of the National Institutes of Health/National Cancer Institute under award number P30CA008748. The content is solely the responsibility of the authors and does not necessarily represent the official views of the National Institutes of Health.

References

1. Marchio C, Weigelt B, Reis-Filho JS. Adenoid cystic carcinomas of the breast and salivary glands (or ‘The strange case of Dr Jekyll and Mr Hyde’ of exocrine gland carcinomas). J Clin Pathol. 2010; 63:220–228. [PubMed: 20203221]

2. Weigelt B, Horlings HM, Kreike B, et al. Refinement of breast cancer classification by molecular characterization of histological special types. J Pathol. 2008; 216:141–150. [PubMed: 18720457]
3. Lakhani, SR.; Ellis, IO.; Schnitt, SJ.; Tan, PH.; van de Vijver, MJ. WHO Classification of Tumours of the Breast. IARC; Lyon: 2012.
4. Weigelt B, Reis-Filho JS. Histological and molecular types of breast cancer: is there a unifying taxonomy? Nat Rev Clin Oncol. 2009; 6:718–730. [PubMed: 19942925]
5. Foulkes WD, Smith IE, Reis-Filho JS. Triple-negative breast cancer. N Engl J Med. 2010; 363:1938–1948. [PubMed: 21067385]
6. Yerushalmi R, Hayes MM, Gelmon KA. Breast carcinoma--rare types: review of the literature. Ann Oncol. 2009; 20:1763–1770. [PubMed: 19602565]
7. Papaspyrou G, Hoch S, Rinaldo A, et al. Chemotherapy and targeted therapy in adenoid cystic carcinoma of the head and neck: a review. Head Neck. 2011; 33:905–911. [PubMed: 20652885]
8. Persson M, Andren Y, Mark J, et al. Recurrent fusion of MYB and NFIB transcription factor genes in carcinomas of the breast and head and neck. Proc Natl Acad Sci U S A. 2009; 106:18740–18744. [PubMed: 19841262]
9. Brill LB 2nd, Kanner WA, Fehr A, et al. Analysis of MYB expression and MYB-NFIB gene fusions in adenoid cystic carcinoma and other salivary neoplasms. Mod Pathol. 2011; 24:1169–1176. [PubMed: 21572406]
10. West RB, Kong C, Clarke N, et al. MYB expression and translocation in adenoid cystic carcinomas and other salivary gland tumors with clinicopathologic correlation. Am J Surg Pathol. 2011; 35:92–99. [PubMed: 21164292]
11. Mitani Y, Li J, Rao PH, et al. Comprehensive analysis of the MYB-NFIB gene fusion in salivary adenoid cystic carcinoma: Incidence, variability, and clinicopathologic significance. Clin Cancer Res. 2010; 16:4722–4731. [PubMed: 20702610]
12. Ho AS, Kannan K, Roy DM, et al. The mutational landscape of adenoid cystic carcinoma. Nat Genet. 2013; 45:791–798. [PubMed: 23685749]
13. Stephens PJ, Davies HR, Mitani Y, et al. Whole exome sequencing of adenoid cystic carcinoma. J Clin Invest. 2013; 123:2965–2968. [PubMed: 23778141]
14. Wetterskog D, Lopez-Garcia MA, Lambros MB, et al. Adenoid cystic carcinomas constitute a genomically distinct subgroup of triple-negative and basal-like breast cancers. J Pathol. 2012; 226:84–96. [PubMed: 22015727]
15. Wetterskog D, Wilkerson PM, Rodrigues DN, et al. Mutation profiling of adenoid cystic carcinomas from multiple anatomical sites identifies mutations in the RAS pathway, but no KIT mutations. Histopathology. 2013; 62:543–550. [PubMed: 23398044]
16. D'Alfonso TM, Mosquera JM, MacDonald TY, et al. MYB-NFIB gene fusion in adenoid cystic carcinoma of the breast with special focus paid to the solid variant with basaloid features. Hum Pathol. 2014; 45:2270–2280. [PubMed: 25217885]
17. Persson M, Andren Y, Moskaluk CA, et al. Clinically significant copy number alterations and complex rearrangements of MYB and NFIB in head and neck adenoid cystic carcinoma. Genes Chromosomes Cancer. 2012; 51:805–817. [PubMed: 22505352]
18. Shah SP, Roth A, Goya R, et al. The clonal and mutational evolution spectrum of primary triple-negative breast cancers. Nature. 2012; 486:395–399. [PubMed: 22495314]
19. The Cancer Genome Atlas Network. Comprehensive molecular portraits of human breast tumours. Nature. 2012; 490:61–70. [PubMed: 23000897]
20. Horlings HM, Weigelt B, Anderson EM, et al. Genomic profiling of histological special types of breast cancer. Breast Cancer Res Treat. 2013; 142:257–269. [PubMed: 24162157]
21. Elston CW, Ellis IO. Pathological prognostic factors in breast cancer. I. The value of histological grade in breast cancer: experience from a large study with long-term follow-up. Histopathology. 1991; 19:403–410. [PubMed: 1757079]
22. Piscuoglio S, Ng CK, Martelotto LG, et al. Integrative genomic and transcriptomic characterization of papillary carcinomas of the breast. Mol Oncol. 2014; 8:1588–1602. [PubMed: 25041824]
23. Hammond ME, Hayes DF, Dowsett M, et al. American Society of Clinical Oncology/College Of American Pathologists guideline recommendations for immunohistochemical testing of estrogen

and progesterone receptors in breast cancer. J Clin Oncol. 2010; 28:2784–2795. [PubMed: 20404251]

24. Wolff AC, Hammond ME, Hicks DG, et al. Recommendations for human epidermal growth factor receptor 2 testing in breast cancer: American Society of Clinical Oncology/College of American Pathologists clinical practice guideline update. J Clin Oncol. 2013; 31:3997–4013. [PubMed: 24101045]
25. Fusco N, Colombo P-E, Martelotto LG, et al. Resolving quandaries: basaloid adenoid cystic carcinoma or breast cylindroma? The role of massively parallel sequencing. Histopathology. 2015 Epub ahead of print. 10.1111/his.12735
26. Fehr A, Kovacs A, Loning T, et al. The MYB-NFIB gene fusion-a novel genetic link between adenoid cystic carcinoma and dermal cylindroma. J Pathol. 2011; 224:322–327. [PubMed: 21618541]
27. Weinreb I, Piscuoglio S, Martelotto LG, et al. Hotspot activating PRKD1 somatic mutations in polymorphous low-grade adenocarcinomas of the salivary glands. Nat Genet. 2014; 46:1166–1169. [PubMed: 25240283]
28. Li H, Durbin R. Fast and accurate long-read alignment with Burrows-Wheeler transform. Bioinformatics. 2010; 26:589–595. [PubMed: 20080505]
29. McKenna A, Hanna M, Banks E, et al. The Genome Analysis Toolkit: a MapReduce framework for analyzing next-generation DNA sequencing data. Genome Res. 2010; 20:1297–1303. [PubMed: 20644199]
30. Cibulskis K, Lawrence MS, Carter SL, et al. Sensitive detection of somatic point mutations in impure and heterogeneous cancer samples. Nat Biotechnol. 2013; 31:213–219. [PubMed: 23396013]
31. Koboldt DC, Zhang Q, Larson DE, et al. VarScan 2: somatic mutation and copy number alteration discovery in cancer by exome sequencing. Genome Res. 2012; 22:568–576. [PubMed: 22300766]
32. Saunders CT, Wong WS, Swamy S, et al. Strelka: accurate somatic small-variant calling from sequenced tumor-normal sample pairs. Bioinformatics. 2012; 28:1811–1817. [PubMed: 22581179]
33. Narzisi G, O'Rawe JA, Iossifov I, et al. Accurate de novo and transmitted indel detection in exome-capture data using microassembly. Nat Methods. 2014; 11:1033–1036. [PubMed: 25128977]
34. Thorvaldsdottir H, Robinson JT, Mesirov JP. Integrative Genomics Viewer (IGV): high-performance genomics data visualization and exploration. Brief Bioinform. 2013; 14:178–192. [PubMed: 22517427]
35. Schwarz JM, Rodelsperger C, Schuelke M, et al. MutationTaster evaluates disease-causing potential of sequence alterations. Nat Methods. 2010; 7:575–576. [PubMed: 20676075]
36. Carter H, Chen S, Isik L, et al. Cancer-specific high-throughput annotation of somatic mutations: computational prediction of driver missense mutations. Cancer Res. 2009; 69:6660–6667. [PubMed: 19654296]
37. Martelotto LG, Ng C, De Filippo MR, et al. Benchmarking mutation effect prediction algorithms using functionally validated cancer-related missense mutations. Genome Biol. 2014; 15:484. [PubMed: 25348012]
38. Kamburov A, Stelzl U, Lehrach H, et al. The ConsensusPathDB interaction database: 2013 update. Nucleic Acids Res. 2013; 41:D793–800. [PubMed: 23143270]
39. Mermel CH, Schumacher SE, Hill B, et al. GISTIC2.0 facilitates sensitive and confident localization of the targets of focal somatic copy-number alteration in human cancers. Genome Biol. 2011; 12:R41. [PubMed: 21527027]
40. Carter SL, Cibulskis K, Helman E, et al. Absolute quantification of somatic DNA alterations in human cancer. Nat Biotechnol. 2012; 30:413–421. [PubMed: 22544022]
41. Lawrence MS, Stojanov P, Polak P, et al. Mutational heterogeneity in cancer and the search for new cancer-associated genes. Nature. 2013; 499:214–218. [PubMed: 23770567]
42. Futreal PA, Coin L, Marshall M, et al. A census of human cancer genes. Nat Rev Cancer. 2004; 4:177–183. [PubMed: 14993899]
43. Kandoth C, McLellan MD, Vandin F, et al. Mutational landscape and significance across 12 major cancer types. Nature. 2013; 502:333–339. [PubMed: 24132290]

44. Lawrence MS, Stojanov P, Mermel CH, et al. Discovery and saturation analysis of cancer genes across 21 tumour types. Nature. 2014; 505:495–501. [PubMed: 24390350]
45. Gao J, Aksoy BA, Dogrusoz U, et al. Integrative analysis of complex cancer genomics and clinical profiles using the cBioPortal. Sci Signal. 2013; 6:pl1. [PubMed: 23550210]
46. Turner N, Lambros MB, Horlings HM, et al. Integrative molecular profiling of triple negative breast cancers identifies amplicon drivers and potential therapeutic targets. Oncogene. 2010; 29:2013–2023. [PubMed: 20101236]
47. El-Rifai W, Rutherford S, Knuutila S, et al. Novel DNA copy number losses in chromosome 12q12--q13 in adenoid cystic carcinoma. Neoplasia. 2001; 3:173–178. [PubMed: 11494110]
48. Turner NC, Reis-Filho JS. Tackling the diversity of triple-negative breast cancer. Clin Cancer Res. 2013; 19:6380–6388. [PubMed: 24298068]
49. Gerlinger M, Rowan AJ, Horswell S, et al. Intratumor heterogeneity and branched evolution revealed by multiregion sequencing. N Engl J Med. 2012; 366:883–892. [PubMed: 22397650]
50. de Bruin EC, McGranahan N, Mitter R, et al. Spatial and temporal diversity in genomic instability processes defines lung cancer evolution. Science. 2014; 346:251–256. [PubMed: 25301630]
51. Alexandrov LB, Nik-Zainal S, Wedge DC, et al. Signatures of mutational processes in human cancer. Nature. 2013; 500:415–421. [PubMed: 23945592]

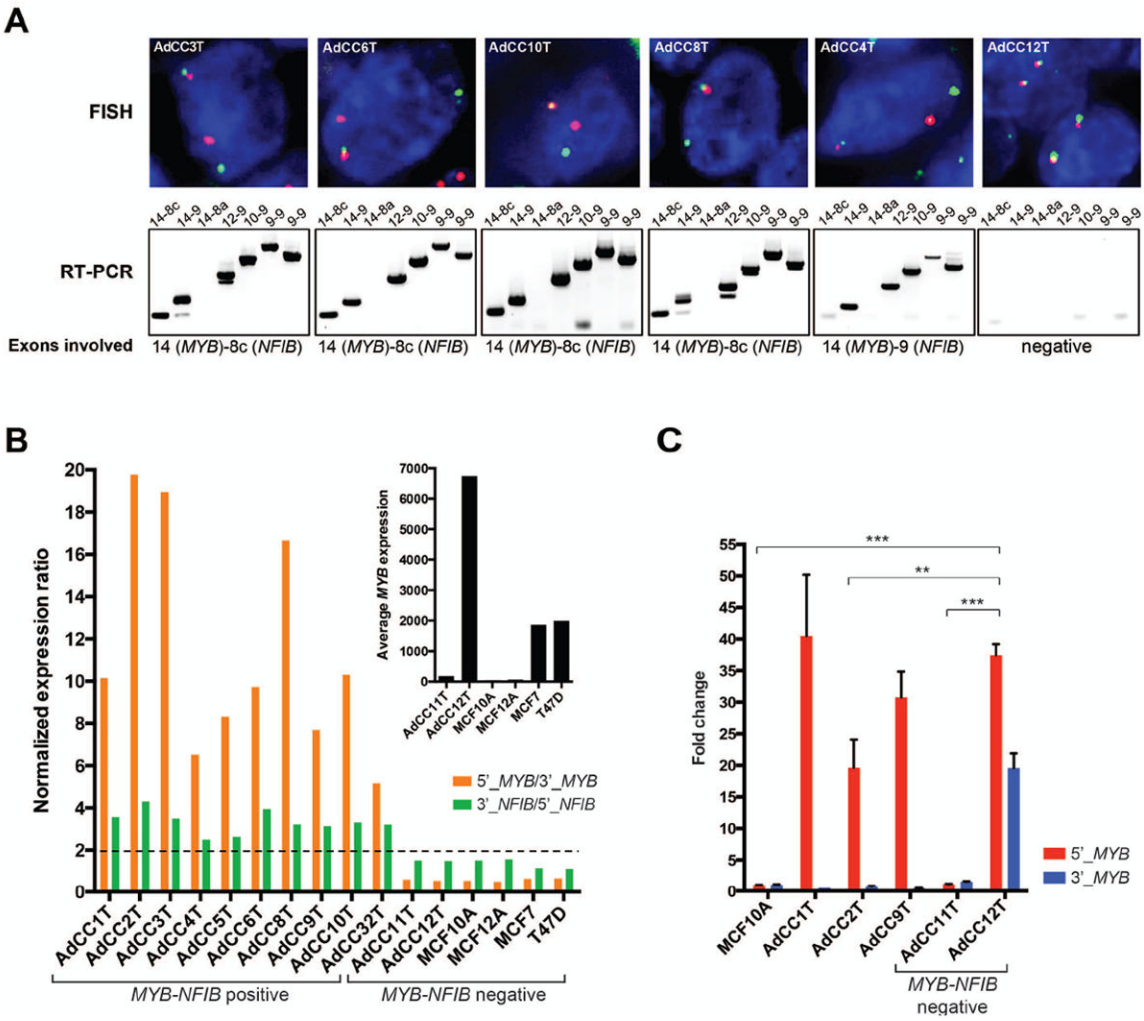

Figure 1. Detection of the *MYB-NFIB* fusion gene and *MYB* and *NFIB* expression in breast AdCCs

(A), Representative FISH micrographs and results of RT-PCR. A *MYB* dual color break-apart probe (top panel) was employed for FISH, where the green and the red probes are proximal and distal to the *MYB* breakpoint cluster region, respectively. The *MYB-NFIB* fusion transcripts (bottom panel) were detected using primers located in *MYB* exons 9, 10, 12 and 14, and in *NFIB* exons 8a, 8c and 9; lane names indicate the respective exons tested. In AdCC12T, neither a *MYB* split signal nor a *MYB-NFIB* fusion transcript could be identified. For the RT-PCR results of the remaining cases, see Supplementary Figure S2. (B) Normalized mRNA expression ratios of 5'*_MYB(exons1-2)*/3'*_MYB(3'UTR)* and 3'*_NFIB(3'UTR)*/5'*_NFIB(exons5-6)* for all breast AdCCs defined by digital gene expression. Controls included RNA derived from MCF10A and MCF12A breast epithelial cells (negative for *MYB* and *MYB-NFIB* fusion mRNA expression), and from T47D and MCF7 ER-positive breast cancer cell lines (positive for *MYB* and negative for *MYB-NFIB* fusion mRNA expression). Dotted line, 2-fold expression difference. Inset illustrating the average between 5' and 3' signals of *MYB* mRNA expression in the *MYB-NFIB* fusion gene-negative tumors AdCC11T and AdCC12T and in cell line controls. (C) Representative

quantitative RT-PCR analysis of expression of 5’ and 3’ regions of *MYB* mRNA in 3 *MYB-NFIB* fusion gene-positive and the 2 *MYB-NFIB* fusion gene-negative AdCCs, and MCF10A cell line control. P-values, one-way ANOVA, Bonferroni’s multiple comparison correction, alpha: 0.05. **p<0.01, ***p<0.001. Error bars, s.d. of the mean (n=3 experimental replicates).

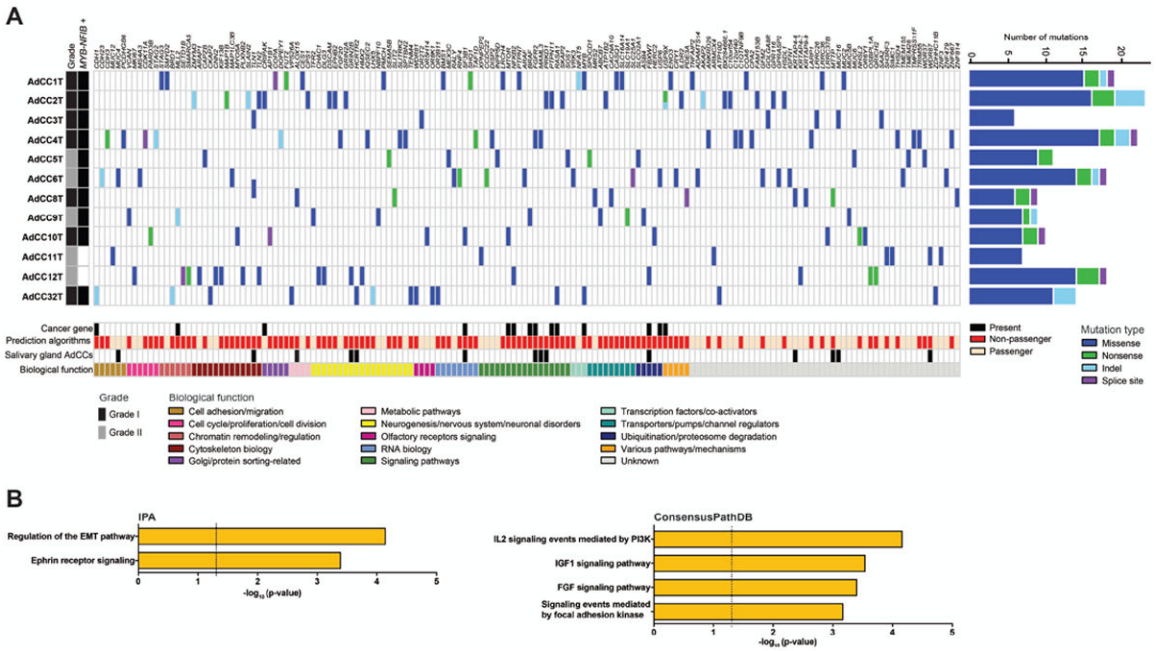

Figure 2. Spectrum of somatic mutations in breast AdCCs

(A) Matrix of all validated and high-confidence somatic mutations identified in 12 breast AdCCs, color-coded by mutation type. The number of mutations identified per case is indicated on the right, and the histologic grade and *MYB-NFIB* fusion gene status on the left. Somatic mutations were classified according to their biological function, and the membership of each gene in cancer gene datasets (Kandoth *et al*. [43], Cancer Gene Census [42] and Lawrence *et al.* [44]). The results of mutation effect prediction algorithms [35-37], and the mutation status in salivary gland AdCCs [12,13] are also shown. (B) Pathways enriched for genes targeted by somatic non-passenger mutations in breast AdCCs, as defined by Ingenuity Pathway Analysis (IPA, left) and ConsensusPathDB [38] (right). Log values of the Benjamini-Hochberg corrected p-value (IPA) and of the hypergeometric test p-value (ConsensusPathDB) are shown.

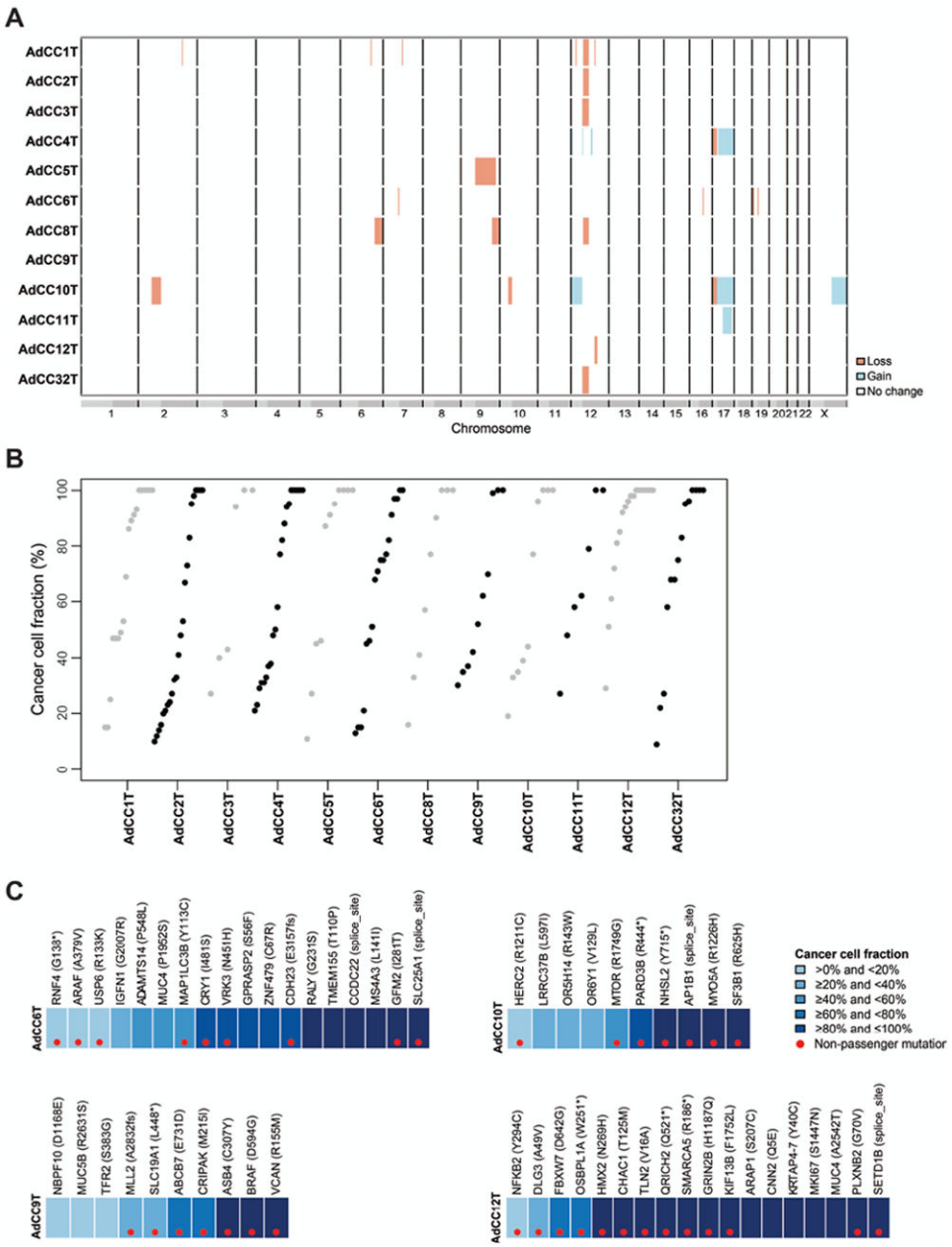

Figure 3. Copy number alterations and clonal mutation frequencies in breast AdCCs

(A) Copy number profiles of breast AdCCs. The genomic position is plotted along the x-axis and the samples on the y-axis. No amplifications and homozygous deletions were found. AdCCs harbored recurrent losses of 12q12-q14.1 and gains of 17q21-q25.1. Orange, copy number loss, blue, copy number gain, white, no copy number change. (B) Clonal frequencies of mutations in breast AdCCs as defined by ABSOLUTE [40] through integration of tumor cellularity, ploidy, gene copy number and mutation data. While all cases harbored clonal mutations (cancer cell fraction ≥80%), validated subclonal mutations were also identified. (C) Representative clonal frequency plots of breast AdCCs as defined by ABSOLUTE [40] through integration of tumor cellularity, ploidy, gene copy number and

mutation data. Cancer cell fractions according to the color-coding in the legend. Red dots represent likely non-passenger mutations.

Table 1

Molecular features of breast AdCCs included in this study.

Case ID	*MYB* rearrangement (FISH)	MYB-NFIB fusion transcript (RT-PCR)	Non-synonymous mutations (n)	Selected gene copy number alterations
AdCC1T	yes	*MYB* Exon 14 – *NFIB* Exon 8c	19	12q12-q14.1 loss
AdCC2T	yes	MYB Exon 9 – NFIB Exon 8c	23	12q12-q14.1 loss
AdCC3T	yes	*MYB* Exon 14 – *NFIB* Exon 8c	6	12q12-q14.1 loss
AdCC4T	yes	*MYB* Exon 14 – *NFIB* Exon 9	22	17q21-q25.1 gain; 17p13.3-p11.2 loss
AdCC5T	no	*MYB* Exon 14 – *NFIB* Exon 9	11	9q13-q34.2 loss
AdCC6T	yes	*MYB* Exon 14 – *NFIB* Exon 8c	18	
AdCC8T	yes	*MYB* Exon 14 – *NFIB* Exon 8c	9	12q12-q14.1 loss
AdCC9T	yes	*MYB* Exon 14 – *NFIB* Exon 9	10	
AdCC10T	yes	*MYB* Exon 14 – *NFIB* Exon 8c	10	17q21-q25.1 gain; 17p13.3-p11.2 loss
AdCC11T	no	not detectable	7	17q21-q25.1 gain
AdCC12T	no	not detectable	18	
AdCC32T	yes	*MYB* Exon 14 – *NFIB* Exon 8c	14	12q12-q14.1 loss

FISH, fluorescence *in situ* hybridization; n, number; RT-PCR, reverse transcriptase PCR.